



A Landsat time series approach to characterize bark beetle and defoliator impacts on tree mortality and surface fuels in conifer forests

Garrett W. Meigs^{a,*}, Robert E. Kennedy^a, Warren B. Cohen^b

^a Department of Forest Ecosystems and Society, Oregon State University, 321 Richardson Hall, Corvallis, OR, 97331, USA

^b Pacific Northwest Research Station, USDA Forest Service, 3200 SW Jefferson Way, Corvallis, OR, 97331, USA

ARTICLE INFO

Article history:

Received 17 February 2011

Received in revised form 9 September 2011

Accepted 10 September 2011

Available online 19 October 2011

Keywords:

Bark beetle

Change detection

Defoliator

Fire

Fuel

Insect disturbance

Landsat time series

Mountain pine beetle

Pacific Northwest

Spectral trajectory

Western spruce budworm

ABSTRACT

Insects are important forest disturbance agents, and mapping their effects on tree mortality and surface fuels represents a critical research challenge. Although various remote sensing approaches have been developed to monitor insect impacts, most studies have focused on single insect agents or single locations and have not related observed changes to ground-based measurements. This study presents a remote sensing framework to (1) characterize spectral trajectories associated with insect activity of varying duration and severity and (2) relate those trajectories to ground-based measurements of tree mortality and surface fuels in the Cascade Range, Oregon, USA. We leverage a Landsat time series change detection algorithm (LandTrendr), annual forest health aerial detection surveys (ADS), and field measurements to investigate two study landscapes broadly applicable to conifer forests and dominant insect agents of western North America. We distributed 38 plots across multiple forest types (ranging from mesic mixed-conifer to xeric lodgepole pine) and insect agents (defoliator [western spruce budworm] and bark beetle [mountain pine beetle]). Insect effects were evident in the Landsat time series as combinations of both short- and long-duration changes in the Normalized Burn Ratio spectral index. Western spruce budworm trajectories appeared to show a consistent temporal evolution of long-duration spectral decline (loss of vegetation) followed by recovery, whereas mountain pine beetle plots exhibited both short- and long-duration spectral declines and variable recovery rates. Although temporally variable, insect-affected stands generally conformed to four spectral trajectories: short-duration decline then recovery, short- then long-duration decline, long-duration decline, long-duration decline then recovery. When comparing remote sensing data with field measurements of insect impacts, we found that spectral changes were related to cover-based estimates (tree basal area mortality [$R^2_{\text{adj}} = 0.40$, $F_{1,34} = 24.76$, $P < 0.0001$] and down coarse woody detritus [$R^2_{\text{adj}} = 0.29$, $F_{1,32} = 14.72$, $P = 0.0006$]). In contrast, ADS changes were related to count-based estimates (e.g., ADS mortality from mountain pine beetle positively correlated with ground-based counts [$R^2_{\text{adj}} = 0.37$, $F_{1,22} = 14.71$, $P = 0.0009$]). Fine woody detritus and forest floor depth were not well correlated with Landsat- or aerial survey-based change metrics. By characterizing several distinct temporal manifestations of insect activity in conifer forests, this study demonstrates the utility of insect mapping methods that capture a wide range of spectral trajectories. This study also confirms the key role that satellite imagery can play in understanding the interactions among insects, fuels, and wildfire.

© 2011 Elsevier Inc. All rights reserved.

1. Introduction

In western North America, native defoliators and bark beetles cause pervasive, regional-scale tree mortality, a profound ecosystem impact that varies from year to year but may be increasing (Raffa et al., 2008; Swetnam & Lynch, 1993). Tree-killing insects influence forest structure and function directly, and they also may influence other forest disturbances, particularly wildfire. Abiotic and biotic factors, including drought, tree condition (e.g., density, age, vigor),

and landscape contiguity, render many forests susceptible to both insect and wildfire disturbances. This co-occurrence of insects and wildfire, coupled with recent and predicted increases in both disturbances due to climate change (Balshi et al., 2009; Bentz et al., 2010; Kurz et al., 2008; Littell et al., 2010; Logan et al., 2003; Raffa et al., 2008; Westerling et al., 2006), raises concerns that insect-caused tree mortality may increase the likelihood of extreme fire behavior and may amplify disturbance interactions (Geiszler et al., 1980; Negron et al., 2008; Simard et al., 2011). To date, however, studies indicate that insect effects on tree mortality, fuels, and fire can diverge widely, depending on forest type, insect type, time since outbreak, vegetation response, fire weather, and fire suppression (e.g., Fleming et al., 2002; Hummel & Agee, 2003; Lynch & Moorcroft, 2008; Page & Jenkins,

* Corresponding author. Tel.: +1 541 758 7758; fax: +1 541 737 1393.

E-mail address: garrett.meigs@oregonstate.edu (G.W. Meigs).

2007b; Simard et al., 2011). A key impediment to better understanding insect–fire interactions is the lack of empirical maps that track both insects and fire consistently over space and time. Although mapping fire with remote sensing approaches is well-established (e.g., Eidenshink et al., 2007), the science of mapping insect effects is relatively nascent.

Previous remote sensing studies have employed a variety of datasets and approaches to map insect disturbance. At broad spatial extents, MODIS-based algorithms are emerging for the detection of insect effects (e.g., Verbesselt et al., 2009), but for many resource-based goals, finer-grained data are required (Cohen & Goward, 2004). Numerous studies have targeted bark beetle outbreaks (mountain pine beetle [*Dendroctonus ponderosae* Hopkins]) in British Columbia (e.g., Coops et al., 2006; Goodwin et al., 2008, 2010) and the U.S. Rocky Mountains (e.g., Lynch et al., 2006; Dennison et al., 2010), using diverse remote sensing datasets, including aerial sketch mapping and photography, Hyperion, Quickbird, GeoEye-1, ASTER, and Landsat (Dennison et al., 2010; Wulder et al., 2006). Many approaches conceptualize insect outbreak stages as relatively abrupt, short-term anomalies from stable forest conditions. Accordingly, a time series of spectral values (hereafter ‘spectral trajectory’) is expected to demonstrate a period of relative spectral stability followed by an abrupt change in spectral value. For example, Goodwin et al. (2008) used a decision tree approach with a temporal sequence of Landsat imagery to identify abrupt changes in the Normalized Difference Moisture Index associated with the onset of mountain pine beetle outbreaks (red attack stage) in north-central British Columbia, achieving >70% accuracy. Yet, insects do not consistently cause abrupt changes in spectral trajectories. Vogelmann et al. (2009) observed relatively long-term, gradual declines in vegetation-based spectral indices on water-stressed slopes in New Mexico, attributing the spectral trajectories to defoliation by western spruce budworm (*Choristoneura occidentalis* Freeman). Indeed, Goodwin et al. (2010) further examined mountain pine beetle effects in British Columbia, developing mixed linear models to characterize the spectral variability occurring over several years of progressive beetle attack. Thus, recent studies suggest that the temporal dynamics of insect disturbance—and the associated spectral trajectories—can vary considerably. To map defoliator and bark beetle impacts consistently across large geographic areas, remote sensing algorithms must characterize the full variation of spectral trajectories.

In addition, to be useful in understanding potential insect and fire interactions, insect mapping must move toward quantifying tree mortality and how that mortality relates to fuel dynamics. Unlike timber harvest, which removes vegetation from a site, insect-related mortality transforms the condition and arrangement of plant material (i.e., fuels) in place. In conifer forests of western North America, bark beetle outbreaks can induce relatively rapid tree mortality and associated foliage color change from green to red, lagged shedding of foliage, bark, and branches, and eventual tree fall (e.g., Klutsch et al., 2009; Page & Jenkins, 2007a; Simard et al., 2011). When western spruce budworm defoliation persists for several consecutive years, it also can result in widespread tree mortality (often in conjunction with bark beetles; Goheen & Willhite, 2006; Hummel & Agee, 2003; Vogelmann et al., 2009). This insect-caused tree mortality alters canopy fuel moisture and eventually transfers fuels from canopy to surface strata, namely forest floor (litter and duff), fine woody detritus, and down coarse woody detritus (Brown et al., 1982). As canopy, ladder, and surface fuel distributions change, potential fire behavior and fire effects shift accordingly (e.g., Page & Jenkins, 2007b). Empirical testing of this interaction, however, requires pre-fire maps distinguishing insect-caused fuel accumulations. It is unclear from existing remote sensing studies how insect-induced spectral trajectories are related to key biophysical drivers on the ground.

To improve generalized mapping of insect-related effects in forests, this study integrates a Landsat time series change detection algorithm

(LandTrendr; Kennedy et al., 2010), annual forest health aerial detection surveys, and ground-based measurements to investigate cumulative insect impacts on tree mortality and surface fuels in conifer forests. The overall goal is to advance a remote sensing framework to capture the effects of multiple insect agents consistently across variable spatial and temporal scales. In this paper, we demonstrate the potential of our approach with a pilot study in conifer forests of the Cascade Range, Oregon, USA. Our specific objectives are to:

1. Characterize spectral trajectories in Landsat time series associated with defoliator and bark beetle disturbances of varying duration and severity;
2. Relate spectral trajectories to ground-based measurements of insect-caused tree mortality and surface fuels to assess biophysical drivers of spectral change.

The Cascade Range is an ideal region to explore the variability of insect impacts during the Landsat era. Ongoing research leverages dense Landsat time series to assess forest disturbance and recovery processes in the Pacific Northwest Region, including insect activity (e.g., Cohen et al., 2010; Kennedy et al., 2010). A complementary regional dataset is the Cooperative Aerial Detection Survey (ADS), where human observers identify a wide variety of disturbances across forested lands of Oregon and Washington annually (K. Sprengel, USDA Forest Service, personal communication). Coinciding with the digitized ADS record (since 1980) and the launch of the TM sensor on Landsat 5 (1984), mountain pine beetle and western spruce budworm outbreaks have affected dry forest landscapes across much of the region, particularly in the eastern Cascade Range of Oregon. Previous studies have characterized endemic and outbreak levels of insect populations in relatively productive mixed-conifer forests and less productive lodgepole pine (*Pinus contorta* Douglas ex Louden; e.g., Franklin et al., 1995; Geiszler et al., 1980; Hummel & Agee, 2003).

2. Methods

2.1. Analytical approach and study areas

Our analysis employed a Landsat time series change detection algorithm (LandTrendr; Kennedy et al., 2010; see below), annual forest health aerial detection surveys (ADS), and field observations to investigate recent insect activity in the eastern Cascade Range, Oregon. Using maps from LandTrendr and ADS as guides, we distributed 38 survey plots across a range of forest conditions (forest type, insect agent type [bark beetle vs. defoliator] and severity, and time since onset of insect outbreak). We then measured tree mortality and surface fuels at these plots to evaluate and interpret the remotely derived disturbance maps.

We focused on two landscapes that have experienced contrasting insect activity according to the ADS (Figs. 1, 2). The generally higher productivity, mixed-conifer forests in the Mt. Hood Zone experienced widespread defoliation by western spruce budworm (WSB), beginning in the mid-1980s and peaking in the early 1990s, followed by sporadic and locally intense mountain pine beetle (MPB) activity in the early 2000s. In contrast, lower productivity lodgepole pine forests in the Cascade Lakes Zone experienced minimal WSB activity due to the lack of suitable host trees but some of the highest cumulative mortality from MPB in the region, beginning in the early 1980s.

Both landscapes are defined by steep environmental gradients. In the Mt. Hood Zone, dominant tree species are Douglas-fir (*Pseudotsuga menziesii* [Mirb.] Franco), grand fir (*Abies grandis* [Douglas ex D. Don] Lindl.), western larch (*Larix occidentalis* Nutt.), ponderosa pine (*Pinus ponderosa* Douglas ex P. Lawson & C. Lawson), and occasional lodgepole pine. Study plot elevation ranges from 1000 to 1600 m. Averaged across study plots, the 32-year (1978–2009) mean annual precipitation is 2250 mm (SD = 475 mm) and mean annual temperature is 5.8 °C (SD = 1.0 °C) (Daly et al., 2002; PRISM Group, Oregon St. Univ., <http://prism.oregonstate.edu>). In the Cascade Lakes Zone, dominant

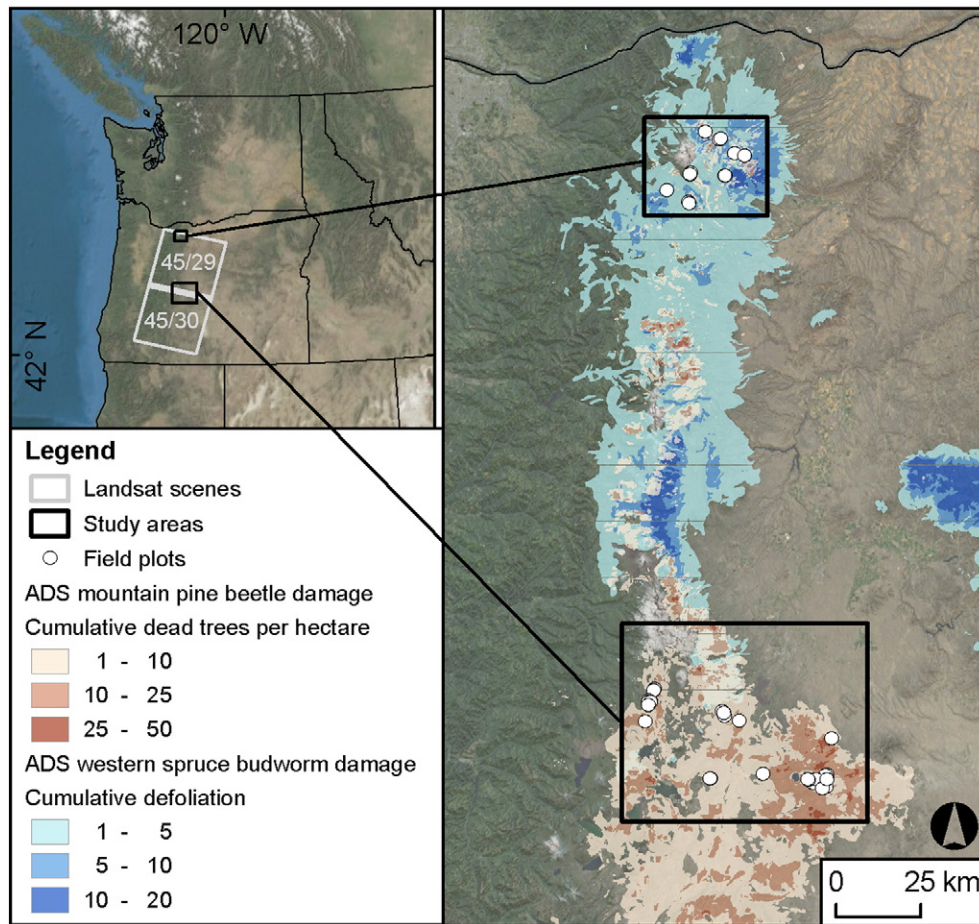


Fig. 1. Study area locations within the Pacific Northwest Region (inset) and Oregon (Landsat scenes 45/29 and 45/30). Insect damage represents cumulative impacts mapped by aerial detection surveys (ADS) from 1980 to 2009. ADS data report mountain pine beetle (MPB; red/brown) damage quantitatively (trees per acre, converted to trees per hectare here) but western spruce budworm (WSB; blue) damage qualitatively on a numeric scale (standardized here to 1–3; see [Methods](#)). MPB data overlap WSB data where the two co-occur, and both are displayed with 30% transparency. Black boxes denote map extents in [Fig. 2](#). Base map: ESRI Imagery World 2D from <http://server.arcgisonline.com>. Projection: Albers NAD83. Note the broad spatial extent of insect disturbance across forests of the Eastern Cascade Range.

tree species at lower elevations are lodgepole pine and ponderosa pine, which intergrade at higher elevations with mixed-conifer species, particularly *Abies spp.*, mountain hemlock (*Tsuga mertensiana* [Bong.] Carrière) and whitebark pine (*Pinus albicaulis* Engelm.). Study plot elevation ranges from 1200 to 2100 m, and 32-year mean annual precipitation and temperature are 895 mm ($SD = 525$ mm) and 5.7 °C ($SD = 0.8$ °C), respectively (<http://prism.oregonstate.edu>). Both study landscapes experience warm, dry summers (Mediterranean climate type), and soils are volcanic in origin (andisols).

2.2. LandTrendr disturbance mapping

We developed maps of forest disturbance and growth using outputs from LandTrendr algorithms and analysis, which are described in detail by [Kennedy et al. \(2010\)](#). Briefly, we acquired georectified, annual Landsat TM/ETM+ images from the USGS Landsat archive for two Landsat scenes that covered our study areas (path 45/rows 29 and 30; [Fig. 1](#)) from 1984 to 2007, with multiple images used in years when clouds obscured part of the study area. We corrected a single image to approximate surface reflectance using the COST approach ([Chavez, 1996](#)) normalized all other images in the same path/row to that reference image using the MADCAL relative radiometric normalization ([Canty et al., 2004](#)), and conducted cloud screening manually. For this temporal stack of normalized Landsat imagery, we then calculated the spectral index referred to as the Normalized Burn Ratio (NBR; [Key &](#)

[Benson, 2006](#)), which contrasts Landsat bands four and seven (near infrared [NIR] and shortwave infrared [SWIR], respectively):

$$NBR = (\text{Band 4} - \text{Band 7}) / (\text{Band 4} + \text{Band 7}) \quad (1)$$

In its contrast between the NIR and SWIR bands, NBR is similar to spectral indices used in other studies to track insect effects (e.g., [Goodwin et al., 2008, 2010](#); [Vogelmann et al., 2009](#); [Wulder et al., 2006](#)). In our study region, NBR is particularly applicable because sensitivity analyses have shown its utility for capturing disturbance processes relative to other indices ([Cohen et al., 2010](#); [Kennedy et al., 2010](#)) and because of its familiarity to the fire science community ([Eidenshink et al., 2007](#)).

Following preparation of the Landsat image stacks, we applied LandTrendr temporal segmentation algorithms to the time series of NBR values at each pixel. Segmentation distills an often-noisy yearly time series into a simplified series of segments to capture the salient features of the trajectory while avoiding most false changes ([Kennedy et al., 2010](#)). We derived disturbance maps at the Landsat pixel scale using key characteristics of these segments. Disturbance segments were defined as those segments experiencing a decline in NBR over time ([Cohen et al., 2010](#); [Kennedy et al., 2010](#)). To minimize commission errors due to background variation and statistical noise, we only accepted segments whose change in NBR exceeded a threshold value of 50 units ($NBR \times 1000$), adjusted to higher values for shorter duration

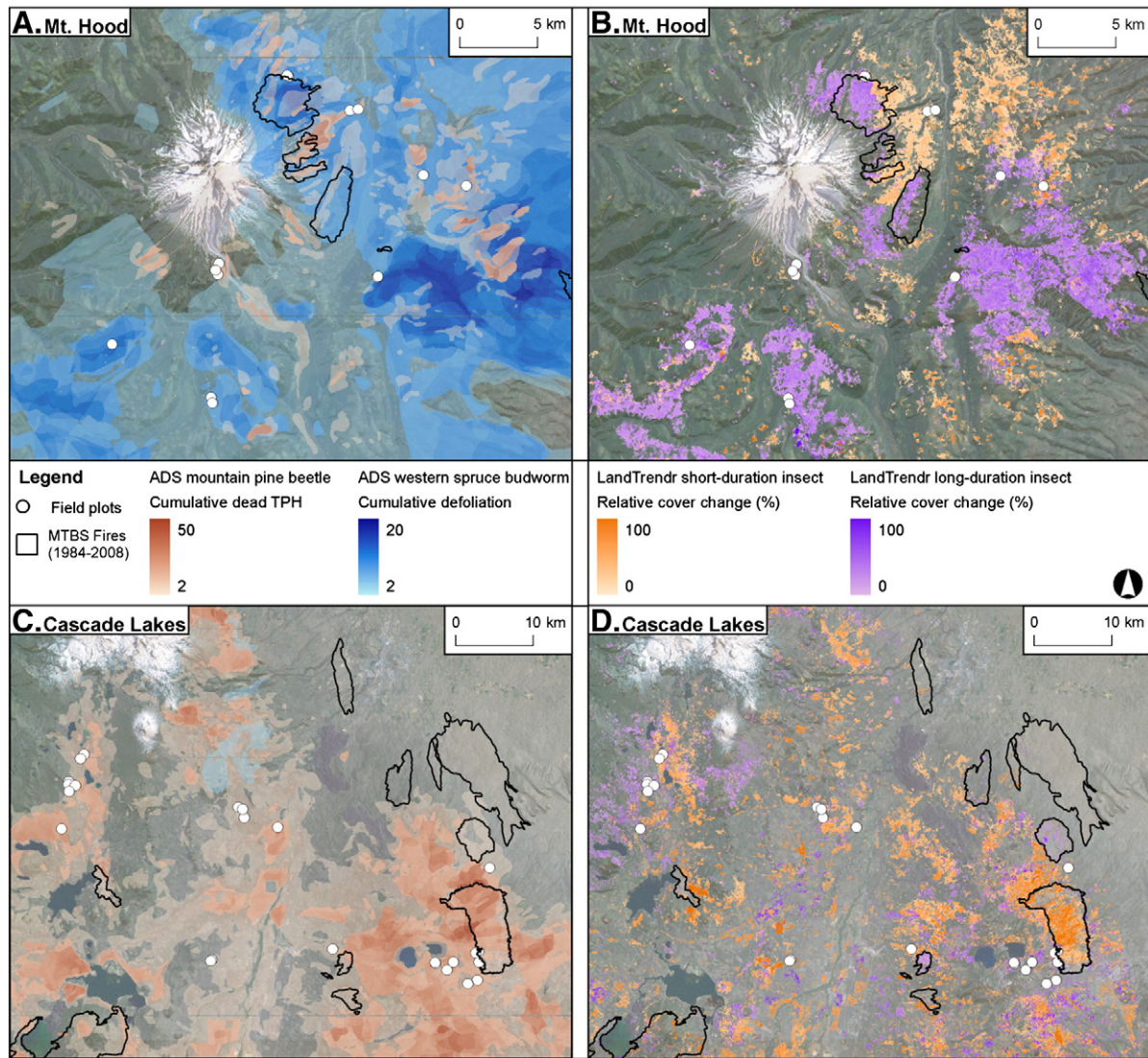


Fig. 2. Aerial detection survey and Landsat-based maps of forest disturbance across study landscapes. Note different spatial extents in two study areas. Panels (A) and (C) show aerial observations of cumulative damage from mountain pine beetle (MPB; red/brown) and western spruce budworm (WSB; blue) from 1980 to 2009 (displayed with 30% transparency; MPB overlaps WSB in A, WSB overlaps MPB in C). Panels (B) and (D) show LandTrendr (Kennedy et al., 2010) maps of the magnitude of short-duration (<6 years) and long-duration (≥6 years) insect disturbance, excluding non-forested areas. Fire perimeters from: <http://mtbs.gov>. Base map: ESRI Imagery World 2D from <http://server.arcgisonline.com>. Projection: Albers NAD83. Note: (1) contrasting recent insect disturbance histories between study landscapes; (2) location of field plots; (3) broad spatial extent of ADS polygons versus the spatially-constrained Landsat pixels; (4) general agreement of heavy insect damage areas among both data sources; (5) Overlap of some but not all fires with insect disturbance areas.

segments. For each disturbance segment, we mapped the absolute change in NBR from start to finish as an estimate of disturbance magnitude. We also mapped the onset year and duration of the segment (in years). We classified the disturbance segments according to whether they were associated with a long-duration decline (defined here as lasting six or more years) or short-duration decline (less than six years). For those segments associated with long-duration trends, we also identified those with evidence of post-disturbance vegetation growth (positive change in NBR) lasting three or more years. These maps were used first to aid in locating field plots (see Section 2.4) and later to characterize disturbance at each field plot (see Section 2.6).

Strictly for the purposes of display (Fig. 2), we derived filtered maps to emphasize disturbances likely caused by insects and to de-emphasize those likely caused by other agents (e.g., logging, fire). The filtering process included a combination of classification algorithms based on training data acquired by trained interpreters, followed by manual removal of overlapping fire perimeters (based on

maps from <http://mtbs.gov>). The filtered maps were not intended as a final mapping product but rather to show the potential of Landsat time series data to map insect impacts.

2.3. Aerial detection survey mapping

Since the mid-twentieth century, state and federal agencies have conducted annual aerial surveys of forested lands in Oregon and Washington (USDA Forest Service Region 6). Human observers identify a wide variety of biotic and abiotic forest disturbances, including insect and disease impacts on specific host tree species (Ciesla, 2006, K. Sprengel, USDA Forest Service, personal communication). Observations were recorded as thematic polygons, digitized versions of which are available since 1980 (<http://www.fs.fed.us/r6/nr/fid/as>). We used this multiple decade record to identify insect agents associated with LandTrendr disturbance segments.

We also used the ADS record to extract cumulative insect effects for comparison with LandTrendr outputs and field data, enabling us to assess the robustness of the ADS dataset. We converted all ADS data from 1980 to 2009 into raster format (30 m grain size) and used GIS-type queries in the IDL programming language (<http://www.itvvis.com>) across years in each cell to identify the onset and duration of mountain pine beetle and western spruce budworm. We tallied the total magnitude of each agent's effects, using the quantitative trees per acre count for MPB (converted to trees per hectare) and the qualitative defoliation severity estimate for WSB. The WSB severity data were recorded on a numeric scale (1–4) from 1994 to 1998 and a thematic scale (low, medium, high, and very high) for all other years. We converted the thematic scale to a standard numeric scale (low to 1, medium to 2, high and very high to 3) and summed the severity estimates across all years. Additionally, to derive a common quantitative metric across all plots, we calculated the cumulative duration of both agents observed at each plot.

2.4. Field plot selection

With limited resources for field surveys and with a study focus on description rather than prediction, we used a purposive sampling approach designed to observe quickly a range of conditions across the study zones. Using LandTrendr and ADS maps as guides, we established 38 field plots in September–November 2009 (14 plots in the Mt. Hood Zone, 24 plots in the Cascade Lakes Zone; *Figs. 1, 2*). Because one of our objectives was to describe spectral trajectories associated with insect disturbance and recovery processes, we excluded stands with evidence of substantial anthropogenic activity (e.g., salvage harvest, thinning) or fire occurrence since 1984 (verified via GIS data [<http://mtbs.gov>]). To reduce backcountry travel time, we limited sample points to distances within 1000 m of roads and trails, after determining that pixels closer to roads spanned the same range of remotely sensed insect impacts as all pixels across the study landscapes.

2.5. Field measurements of tree mortality, surface fuels, and landcover

We designed plot-level measurements as a rapid assessment of tree mortality and surface fuel distributions within a single Landsat pixel (30*30 m). At each plot, we quantified live and dead trees in four circular subplots located 14 m from plot center in the sub-cardinal directions (NE, SE, SW, NW; *Fig. A1*). At each subplot, we used variable-radius subplots (prism sweep; basal area factor 10) to estimate live and dead tree basal area and fixed-radius subplots (9 m radius) to estimate live and dead trees per hectare. For direct comparison with aerial detection survey estimates of cumulative tree mortality, we tallied trees in three height strata (dominant, codominant, understory), presenting here the estimates from dominant and codominant strata only. Within the fixed-radius subplots, we also tallied all dead, down trees that were likely rooted within the 9 m radius before being killed by recent insect outbreaks. Although we did not attempt to date the death of individual trees, we classified each down tree based on our confidence that the tree died during the time period identified by ADS data (three confidence levels—90%, 75%, 50%—based on their decay class and evidence of insect disturbance [i.e., bark beetle galleries]). In this paper, we present a conservative estimate of down, dead trees, including only the highest confidence level ($n = 1409/1574$; 90% of sampled down trees).

We measured woody surface fuels along line intercept transects (Brown, 1974; Brown et al., 1982; Harmon & Sexton, 1996) originating at plot center and extending 21 m in the sub-cardinal directions (*Fig. A1*). For down coarse woody detritus (CWD; 1000 hour fuels; all woody pieces ≥ 7.62 cm diameter), we recorded species, diameter (cm), decay class (1–5), and char class (0: no char, 1: bark char; 2:

wood char) along the full transect length (84 m). For fine woody detritus (FWD), we recorded time lapse-based size class (1 h: <0.65 cm; 10 h: 0.65–2.54 cm; 100 h: 2.55–7.62 cm), decay class, and char class along size class-specific segments (1, 10, 100 hour fuels along 12, 24, 84 m, respectively). We converted line intercept counts to volume per unit area using standard equations after Harmon and Sexton (1996) and estimated total CWD and FWD mass with decay class-, species-, and ecoregion-specific wood density values (Hudiburg et al., 2009; Meigs et al., 2009). We sampled ground layer fuels by measuring litter and duff depth at two points along each transect (8 total per plot).

To capture potential insect effects on live overstory and understory fuels at each fixed-area subplot, we completed a standard land-cover classification with ocular estimates of percent cover for each of the following classes: live and dead needleleaf tree, live and dead broad-leaf tree, shrub, herb, light litter/duff, dark litter/duff, and rock/soil. To aid in imagery interpretation, we collected six photographs from each subplot center (24 total per plot).

2.6. Data analysis

We scaled all field measurements to per-unit-area values for comparison among insect agents, forest types, and study areas. At each plot location, we extracted via GIS the onset, duration, and magnitude of change from LandTrendr and ADS maps at the co-occurring pixel (applying no spatial filter). We compared the remotely sensed disturbance magnitude values with our field measurements of tree mortality and surface fuels. We calculated tree basal area percent mortality from the variable-radius plot data, recognizing that this metric would provide an integrated measure of vegetation change for standing trees only. Because the ADS sketch maps identify trees per unit area affected by various mortality agents, we used the fixed-radius overstory dead tree counts to calculate an analogous field-based metric. We related field measurements to remotely sensed indices with simple linear regression (lm procedure; R Development Core Team, 2011). Where appropriate, we subsetted the dataset by study zone (e.g., WSB only prevalent in Mt. Hood Zone) and excluded outlier plots that were not from the sample population of interest in specific statistical comparisons (e.g., old forest plots with high levels of down coarse woody detritus not associated with recent changes). We assessed these relationships with R^2 , adjusted R^2 (R^2_{adj}), P values, and regression coefficients.

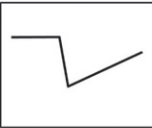
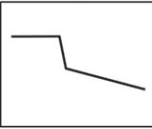
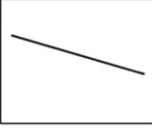
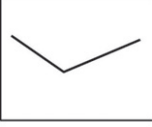
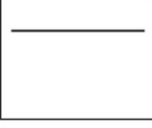

3. Results and discussion

3.1. Spectral trajectories of bark beetles and defoliators

Because previous studies have identified diverse, seemingly disparate temporal signals associated with insect disturbance (e.g., Goodwin et al., 2008, 2010; Vogelmann et al., 2009), we sought to advance a remote sensing framework to capture a variety of spectral trajectories (i.e., temporal trajectories of spectral response to insect activity) objectively and consistently. Across both study zones, the LandTrendr algorithm detected several spectral trajectories at insect disturbance areas identified by aerial detection survey sketch maps. In general, insect effects were evident in the Landsat time series as combinations of both short- and long-duration spectral change. In fact, the majority of plots exhibited long-duration declines (≥ 6 years) in the NBR index, corresponding to relatively slow disturbance processes at an annual time step (*Table 1*). Although study plots were distributed across a broad range of conditions (tree structure and composition, site productivity, insect agent and severity), each plot affected by insect disturbance conformed to one of four generalized spectral trajectories: short-duration decline then recovery, short- then long-duration decline, long-duration decline, and long-duration decline then recovery (*Table 1*). Two additional spectral trajectories not

Table 1

Conceptual framework to characterize spectral trajectories associated with insect activity, stable conditions, and growth.

Spectral trajectory	Interpretation	Insect mortality agent (from ADS, field obs.)	Number of plots (<i>n</i> = 38)			Environmental conditions
			MH	CL	Total	
	Stable, rapid mortality, recovery	Mountain pine beetle	0	4	4	Relatively productive sites
	Stable, rapid mortality, slow mortality	Mountain pine beetle	0	2	2	Multiple disturbance processes such as mortality followed by tree fall
	Long, slow mortality	Mountain pine beetle Western spruce budworm	4	4	8	Long-term presence of insects or multiple insect agents affecting different hosts within a stand
	Slow mortality, recovery	Mountain pine beetle Western spruce budworm	7	6	13	Relatively productive, mesic sites exhibiting rapid recovery following insect disturbance
	Stable (no change)	None	3	3	6	Stable over time interval
	Growth or recovery	Potential prior insect	0	5	5	Potentially linked with natural or anthropogenic disturbance

Notes:

In this study, insect-affected stands generally conformed to the top four generalized spectral trajectories. Our interpretation of these sequences of change and our description of environmental conditions are based on field observations.

Abbreviations: ADS: aerial detection survey; MH: Mt. Hood Zone; CL: Cascade Lakes Zone.

associated with insect mortality—stable and growth—occurred frequently across the study landscapes. Together, these six trajectories represent a conceptual basis for interpreting the most important sequences of change across these dynamic landscapes.

Stands affected by mountain pine beetle (MPB) did not exhibit a single diagnostic disturbance trajectory. Some MPB plots exhibited short-term declines in NBR (e.g., Fig. 3A), but these mortality “events” were often followed by continued declines, suggesting an initial spike in mortality followed by subsequent mortality and dead tree fall. Other MPB plots showed gradually declining NBR (e.g., Fig. 3B), which was sometimes followed by spectral recovery. In general, these plots exhibited relatively lower proportional tree mortality, more robust lodgepole pine regeneration, or higher abundance of non-host species (e.g., *Abies spp.*, *Tsuga mertensiana*) than plots with more abrupt spectral declines. Our findings of both short- and long-duration vegetation decline associated with MPB are consistent with previous studies (e.g., Goodwin et al., 2008, 2010; Wulder et al., 2006) and highlight the diverse effects of bark beetles on forest cover and structure.

In contrast to the high variability in spectral response among mountain pine beetle plots, stands affected by western spruce budworm (WSB) defoliation consistently showed long-duration spectral declines, typically followed by relatively strong spectral recovery (e.g., Fig. 3C). WSB plots occurred only in the Mt. Hood Zone, a landscape characterized by relatively productive mixed-conifer forest compared to the Cascade Lakes Zone. We suggest that the long-duration decline followed by recovery signal is a diagnostic spectral trajectory

for WSB in these mixed-conifer forests, where partial overstory tree survival and understory vegetation growth result in relatively rapid re-greening of defoliated plots. Our observations of gradual spectral changes associated with WSB support the findings of Vogelmann et al. (2009), who documented gradually increasing SWIR/NIR reflectance in New Mexico associated with WSB damage in spruce-fir forests, although they did not have temporal coverage of post-outbreak years that might indicate a vegetation recovery signal.

The observed differences between MPB trajectories (variable combinations of both short- and long-duration disturbance) and WSB trajectories (consistently long-duration disturbance) reflect the distinct biological effects of these two types of insect. Our results show that bark beetles (MPB) can indeed induce rapid forest changes but that their pixel-scale impacts typically evolve over several years. By definition, WSB defoliation takes several consecutive years to yield substantial vegetation mortality, often in conjunction with tree-killing bark beetles in late stages of defoliation (Goheen & Willhite, 2006; Hummel & Agee, 2003). Despite these cumulative impacts, our observation of rapid spectral recovery at WSB sites suggests relatively transient defoliator impacts in these mixed-conifer forests. These results demonstrate that no single model of temporal change can capture the full range of insect-induced changes across heterogeneous landscapes. Instead, remote sensing approaches require: (1) the capacity to detect the full variety of short- and long-duration changes, including both spectral losses and gains; (2) attribution datasets such as ADS and field observations.

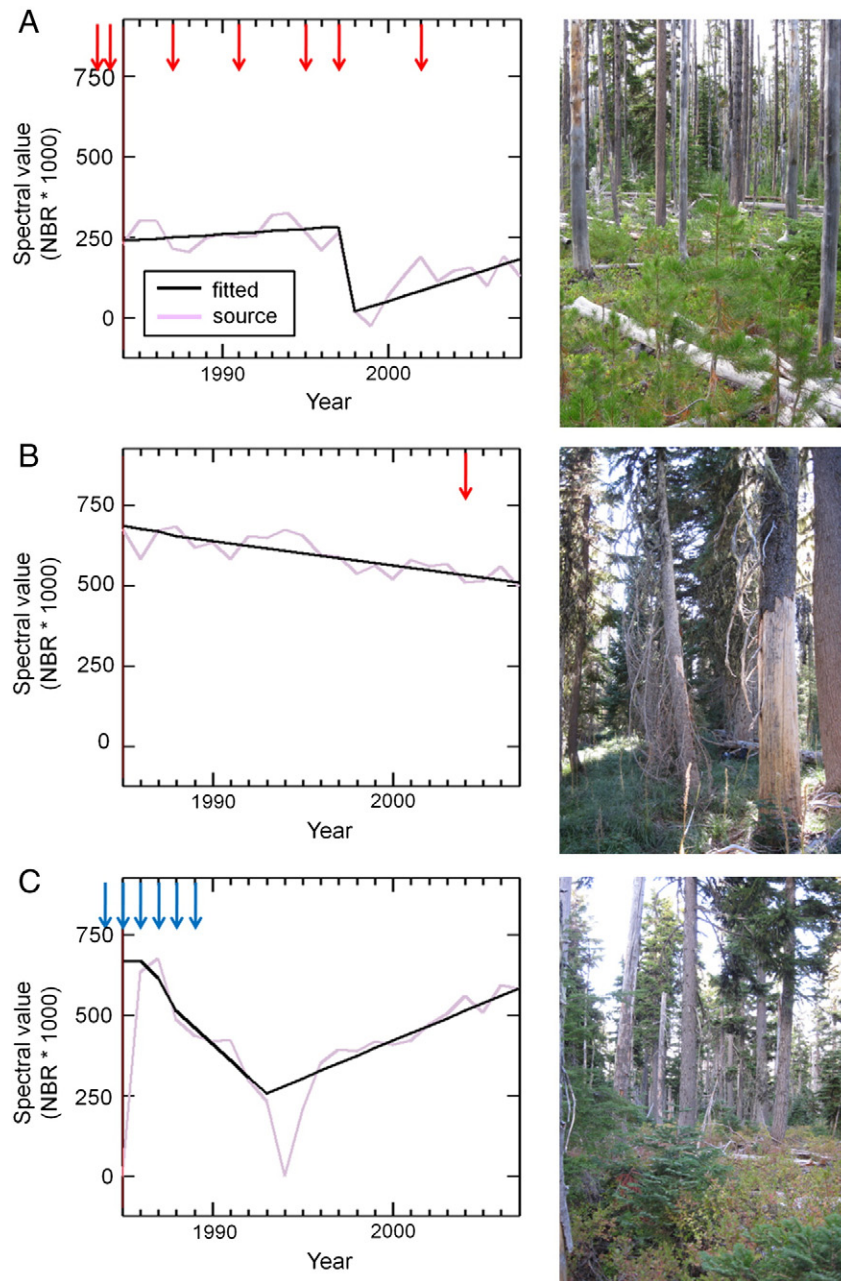


Fig. 3. Example LandTrendr spectral trajectories (Kennedy et al., 2010) and plot photographs. NBR: Normalized Burn Ratio derived from Landsat bands 4 and 7 (Key & Benson, 2006), multiplied by 1000. A: short-duration disturbance followed by spectral recovery. B: long-duration disturbance. C: long-duration disturbance followed by spectral recovery. Zero values in C are from clouds excluded from LandTrendr fits. Vertical arrows indicate aerial detection of insect activity (red: mountain pine beetle; blue: western spruce budworm).

3.2. Spectral trajectory and aerial survey relationships with insect-caused tree mortality and surface fuels

The satellite and aerial survey maps both captured elements of ground-based measurements of insect effects. Across both study landscapes, LandTrendr disturbance magnitude (NBR units) was positively correlated with tree basal area mortality, particularly when two field plots experiencing change outside the Landsat time series interval were excluded ($R^2_{\text{adj}} = 0.40$, $F_{1,34} = 24.76$, $P < 0.0001$; Fig. 4A). Although this relationship indicates that LandTrendr accounts for only a portion of the variation in observed tree mortality, this result is particularly encouraging because field plots were distributed across highly heterogeneous stands and landscapes without replication. In addition, the basal area mortality metric did not capture insect-killed trees that had already fallen at the time of field measurements.

Combining the ADS MPB and WSB into a single metric of cumulative insect presence enabled the direct comparison of the two study landscapes, showing a positive correlation of insect duration with field measurements of dead overstory trees per hectare (TPH; $R^2_{\text{adj}} = 0.26$, $F_{2,35} = 7.38$, $P = 0.002$; Fig. 4B). Similarly, the dead TPH count was positively correlated with the ADS metric of cumulative dead TPH attributed to MPB, particularly in the Cascade Lakes Zone ($R^2_{\text{adj}} = 0.37$, $F_{1,22} = 14.71$, $P = 0.0009$; Fig. 4D), which experienced more intense and pervasive MPB impacts than the Mt. Hood Zone. Although the TPH metrics were positively correlated, the field-based estimates were about one order of magnitude higher than the ADS estimates (Fig. 4D). The cumulative ADS damage from WSB was not well correlated with the number of dead overstory trees per hectare (data not shown), but there did appear to be a threshold effect with tree basal area basal area mortality.

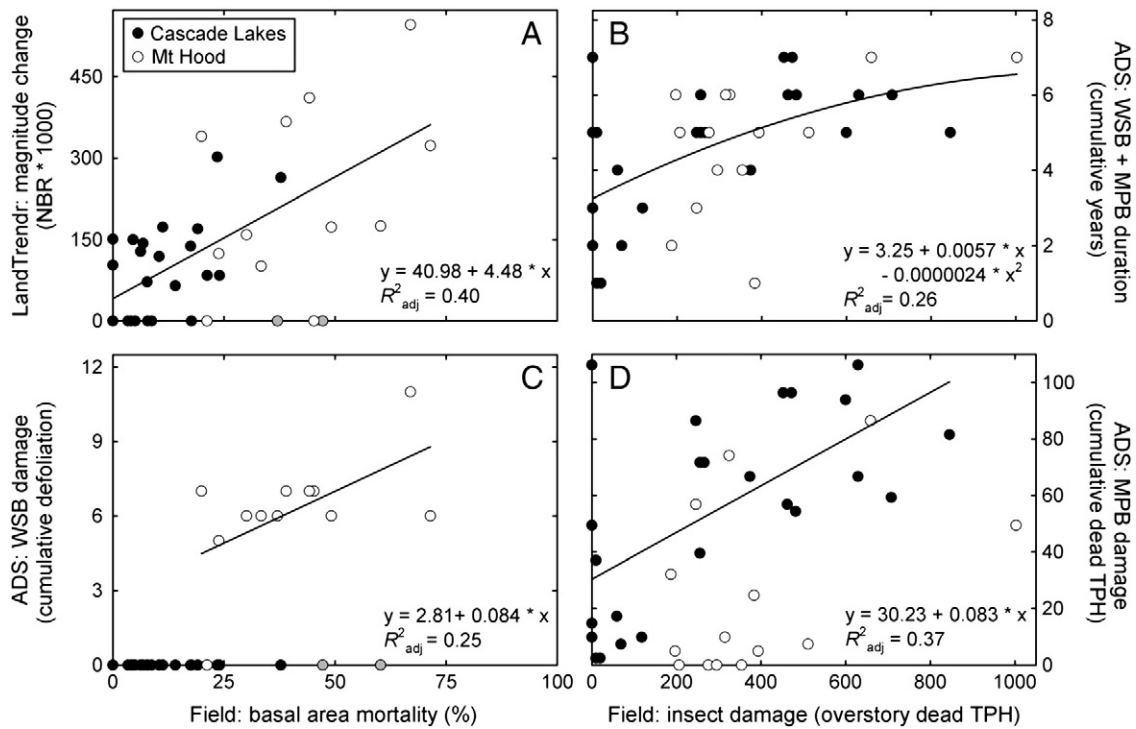


Fig. 4. Relationships of field-measured tree mortality with LandTrendr disturbance (A) and aerial detection survey (ADS) insect maps (B–D). The linear fit in (A) excludes two plots (shown as gray) where disturbance occurred outside of LandTrendr temporal coverage. The quadratic fit in (B) indicates a saturation point (7 years of ADS detection) exceeded by none of the field plots. The linear fit in (C) excludes the Cascade Lakes plots (where minimal WSB occurred) and two additional plots in the Mt. Hood Zone (one where disturbance occurred outside the ADS temporal coverage and one where tree mortality was caused by MPB). The linear fit in (D) excludes the Mt. Hood plots (where MPB impacts were less frequent and intense [Fig. 2]).

Specifically, substantial tree mortality (>20% of basal area) occurred where ADS WSB damage exceeded five units (i.e., for Mt. Hood plots, $R^2_{adj} = 0.25$, $F_{1,10} = 4.72$, $P = 0.055$; Fig. 4C). This result suggests that an appropriate use of the ADS budworm data could be as a presence/absence indicator of heavy defoliation when total impacts exceed the threshold (five damage units). This result also highlights the complementarity of the two remote sensing indices, where ADS sketch maps indicate specific insect agents, and LandTrendr provides a more objective, consistent, quantitative measure of the magnitude of change. Future research could investigate the robustness of this threshold effect.

In contrast to the consistent positive correlations of remotely sensed change maps with overstory tree mortality, the relationships of LandTrendr and ADS change magnitudes with surface fuels were highly

variable (Fig. 5, Table A1). For example, although down coarse woody detritus (CWD) mass was not associated with cumulative ADS presence of MPB and WSB ($R^2_{adj} = -0.03$, $F_{1,34} = 0.13$, $P = 0.721$; Fig. 5A), CWD mass did show a positive correlation with the magnitude of Landsat spectral change (NBR units), particularly when four undisturbed plots were excluded ($R^2_{adj} = 0.29$, $F_{1,32} = 14.72$, $P = 0.0006$; Fig. 5B). This association, in addition to the positive correlation of LandTrendr disturbance magnitude with tree basal area mortality, is consistent with our understanding of the Landsat spectral data being sensitive primarily to vegetative cover (Carlson & Ripley, 1997; Teillet et al., 1997).

To our knowledge, no previous published study has reported a statistically significant relationship between Landsat data and CWD accumulation. CWD accumulation (i.e., snag fall) following

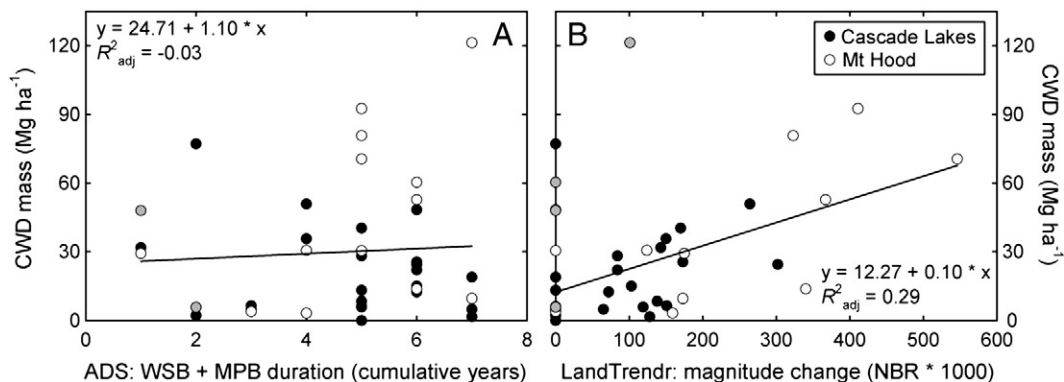


Fig. 5. Relationships of field-measured surface fuels (down coarse woody detritus: CWD) with aerial detection survey (ADS) insect maps (A) and LandTrendr disturbance (B) maps. Gray points indicate plots outside of ADS and LandTrendr temporal coverage.

disturbance is a highly stochastic process that depends on many factors (Russell et al., 2006). For example, Russell et al. (2006) estimated half-lives for standing, fire-killed ponderosa pine and Douglas-fir of 9–10 and 15–16 years, respectively, and Simard et al. (2011) observed a tripling of MPB-killed CWD across a 35 year chronosequence. Klutsch et al. (2009) did not observe significant differences in CWD between stands affected and unaffected by MPB 0–7 years following outbreak, but they did project significant increases of CWD over decadal time scales more applicable to the change maps evaluated in the current study. Similarly, Hummel and Agee (2003) observed a near doubling of CWD after eight years in stands affected by WSB, a time interval consistent with our observations.

Despite evidence of an apparent relationship between LandTrendr disturbance magnitude and CWD, neither LandTrendr nor ADS measures were correlated with fine woody detritus (FWD) or forest floor depth (Table A1), indicating that the cumulative overstory impacts of defoliators and bark beetles did not translate to changes in fine surface fuels. The lack of significant differences in FWD is consistent with field measurements up to seven years following MPB outbreak in Rocky Mt. lodgepole pine forests (Klutsch et al., 2009; Simard et al., 2011), although both studies did document an initial increase in forest floor (litter) depth.

FWD is an important contributor to surface fire behavior (e.g., fire line intensity; Page & Jenkins, 2007b; Simard et al., 2011), whereas CWD is not a key element in surface or crown fire models (Hummel & Agee, 2003). Indeed, although several studies have demonstrated or projected increasing CWD surface fuels following insect outbreaks (e.g., Hummel & Agee, 2003; Klutsch et al., 2009; Simard et al., 2011), these studies have not shown significant increases in simulated crown fire potential. At our study plots, the significant increase in CWD but lack of change in FWD highlights the variability and relatively high levels of fine surface fuels in conifer forests—whether insect affected or not. This result also suggests that insect disturbance may increase potential fire residence time and soil heating associated with CWD but may not influence fire intensity and spread associated with FWD. Future studies should continue to investigate the fuels mechanisms associated with insect outbreak cycles, including the role of live vegetation fuels, which were not assessed in this study. A larger field sample size and replication/stratification likely would result in stronger statistical relationships.

3.3. Limitations and uncertainties

This study presents a promising integration of remote sensing and field observations (see Section 3.4 below). As in any remote sensing investigation, our pilot study was limited by uncertainties associated with each component dataset. For example, the 38 field plots were distributed purposively across diverse landscape gradients, precluding formal replication, and they were measured at only one point in time. As such, the scope of inference is limited to those specific locations and times.

Because insect disturbance processes have been occurring and continue to evolve, maps derived from the LandTrendr and ADS datasets (Figs. 1, 2) represent snapshots of very dynamic landscapes, retrospectively integrating up to three decades of change into a single image. With our Landsat-based approach, mapping insect effects that evolve over several years is not possible until after the event has started, highlighting the need for yearly direct observations (via ADS) or detection alarms with other satellite tools (e.g., MODIS). In addition, the signal of spectral change likely depends on overall site productivity. Higher-productivity sites have more vegetation to lose, potentially improving detectability, but they typically have greater understory vegetation that may dampen the spectral impact of change. These sites also have higher potential for robust growth/recovery signals. Future studies should investigate detectability thresholds along productivity gradients.

ADS sketch maps are rich in information but have important caveats. A single polygon in any given year can be influenced by many factors, including sun angle, phenological variation, observer-to-observer variation, observer fatigue, and the scale of observation (K. Sprengel, USDA Forest Service, personal communication). In addition, polygons are recorded as homogenous patches of insect damage but actually represent heterogeneous mortality at individual trees within polygons (see scale mismatch discussion below). Further, the interannual variability of ADS observations results in sporadic coverage of what may be continuous, long-duration changes (e.g., the contrasting temporal dynamics between ADS and LandTrendr trajectories; Fig. 3). This patchy spatiotemporal coverage is one contributor to the order of magnitude underestimate of ADS cumulative mortality due to MPB relative to ground-based estimates. Another key factor is the mismatch between plane- and ground-based estimates of trees per hectare (particularly in lodgepole pine stands, where ground-measured density can reach 10^4 trees per hectare). Still, as a relative measure of insect effects on tree mortality, the ADS data captured a substantial proportion of the variation in ground-based observations (statistically significant, positive relationships; Fig. 4B–D), and the human observations provided invaluable identification of specific insect agents. To our knowledge, this is the first published study to present direct comparisons between plane-based ADS sketch maps and ground-based observations of tree mortality caused by MPB (but see Nelson et al., 2006 for evaluation of helicopter-based surveys).

Scale mismatch also affects our ability to precisely link field-based measurement to satellite and ADS data. Because of the cost associated with extensive field data collection, we chose to represent approximately one Landsat pixel with our field measurements (Fig. A1). Linking these measurements to a single Landsat pixel is challenging because of inaccuracy in both the field-based positional data and misregistration in any satellite imagery (particularly a time series). Similarly, the ADS data are collected to represent broad spatial extents, and the condition of any single point within the ADS polygons may or may not be representative of the entire polygon. Because these mismatches introduce noise into quantitative relationships among field and remote estimates, the exploratory results reported here are particularly encouraging.

3.4. Implications and recommendations

Despite the limitations described above, this pilot study presents several previously undocumented findings. By advancing a disturbance mapping methodology that consistently identifies spectral trajectories of varying type, duration, and magnitude (LandTrendr; Kennedy et al., 2010), we have established a framework to integrate results from previous studies that used different spectral indices to assess differing insect agents and spatiotemporal scales. This framework enables the detection of seemingly disparate insect impacts due to defoliators and bark beetles (in addition to other disturbances, including fire and logging), while confirming that bark beetles induce both abrupt and gradual tree mortality and growth trajectories. We have also developed new maps to compare stand- and landscape-scale estimates of insect impacts according to multiple remote sensing datasets, showing that the ADS cumulative mortality maps and filtered LandTrendr insect maps reveal similar geographic patterns of change (Fig. 2), particularly across the Mt. Hood landscape. Finally, we have linked these remote sensing datasets with field observations to quantify relationships between spectral trajectories and tree mortality and, to a lesser degree, changes in surface fuels (CWD).

Future studies could build on these initial findings by leveraging larger field datasets covering multiple time intervals, such as the regional forest inventory networks of the Pacific Northwest (e.g., Current Vegetation Survey, Forest Inventory and Analysis). These large databases sample the full gradient of vegetation, insect, and fire conditions, and they also provide valuable locations for satellite

and airphoto interpretation through the TimeSync validation procedure (Cohen et al., 2010). In addition to their systematic spatio-temporal coverage of forested regions, these inventory plots also sample a larger spatial footprint (~1 ha) than the Landsat pixel size (0.09 ha) rapid assessment plots established in the current study. The larger footprint would enable the assessment of the variation and uncertainty among multiple Landsat pixels within patches of insect-killed trees. For further sampling, analysis, prediction, and interpretation, additional geographic datasets, such as the National Land Cover Data set (Vogelmann et al., 2001), biomass, productivity, and elevation maps, could help constrain spectral trajectory analysis to forests that are particularly vulnerable to specific insect agents and temporal sequences of disturbance, as well as determine detectability thresholds, as described above. Through ongoing studies integrating multiple, regional-scale remote sensing and field datasets, we aim to develop insect disturbance maps encompassing a large population of fire events, thus enabling the observation and analysis of a wide range of potential insect-fuel-fire interaction trajectories.

4. Summary

This study investigated spectral trajectories associated with insect disturbance and related those spectral trajectories to ground-based measurements of tree mortality and surface fuels. A Landsat time series segmentation algorithm (LandTrendr; Kennedy et al., 2010) captured both short- and long-duration changes in spectral reflectance, indicating complex temporal dynamics in insect-affected forests. We identified four general spectral trajectories that could be diagnostic of insect disturbance at the 38 conifer forest stands investigated, but future studies should quantify the variation and uncertainty associated with these trajectories at landscape and regional scales. Both LandTrendr and aerial survey estimates of overstory change were related to field measurements of tree mortality. LandTrendr disturbance magnitude was positively, weakly associated with the accumulation

of coarse surface fuels, suggesting the potential for future studies to advance the development of Landsat-based fuel maps. In contrast, neither remote sensing dataset assessed in this study was associated with fine surface fuels, whose high variability suggests limited effects of insects on surface fire intensity. These results highlight the utility of insect mapping methods that capture a wide range of spectral signals and indicate that methods focusing on relatively short-term anomalies may miss substantial spatial and temporal manifestations of insect disturbance. Given the likely increase of fire and insect activity in western North American forests (Littell et al., 2010; Logan et al., 2003; Westerling et al., 2006), the accurate characterization of insect effects on forests, fuels, and subsequent wildfire will become increasingly important.

Acknowledgments

This research was supported by the USDA Forest Service, Forest Health Monitoring (FHM) Evaluation Monitoring, grant no. WC-F-09-2. We thank D. White and F. Gutierrez for field assistance, Z. Yang for LandTrendr analysis and mapping, M. Huso for statistical assistance, and the Deschutes and Mt. Hood National Forests for access to field sites. We are grateful for discussions with H. Maffei, M. Simpson, K. Sprengel, E. Willhite, and other colleagues in the Region 6 FHM program. We acknowledge the insightful comments of three anonymous reviewers. The development and testing of the LandTrendr algorithms reported in this paper were made possible with support of the USDA Forest Service Northwest Forest Plan Effectiveness Monitoring Program, the North American Carbon Program through grants from NASA's Terrestrial Ecology, Carbon Cycle Science, and Applied Sciences Programs, the NASA New Investigator Program, the Office of Science (BER) of the U.S. Department of Energy, and the following Inventory and Monitoring networks of the National Park Service: Southwest Alaska, Sierra Nevada, Northern Colorado Plateau, and Southern Colorado Plateau.

Appendix A

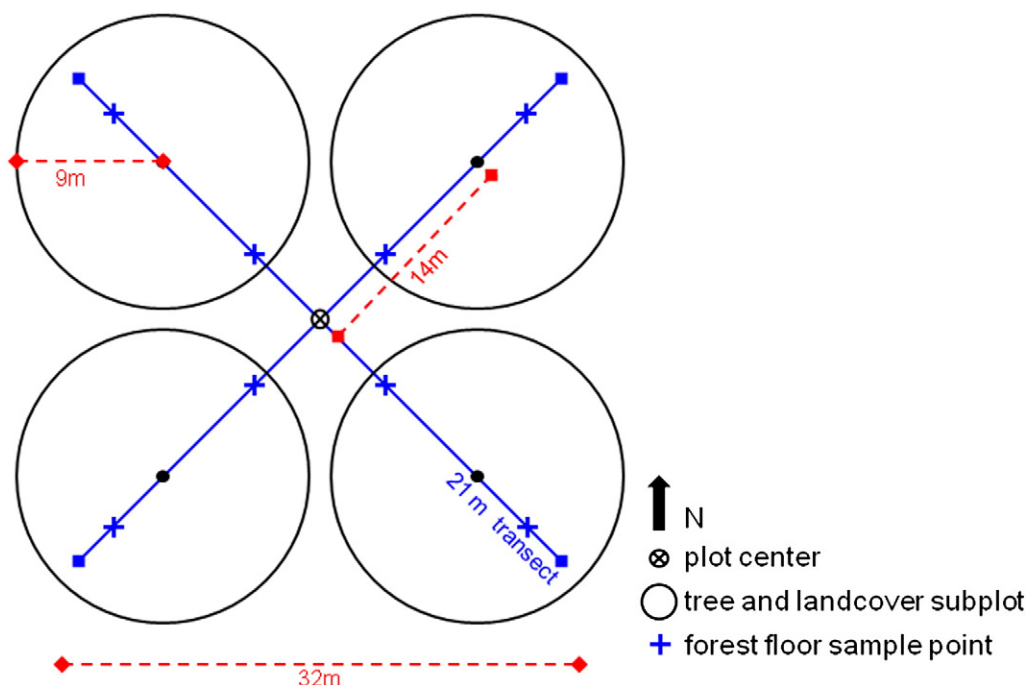


Fig. A1. Field plot sampling design. Notes: The subplots (black circles) and fuels transects (blue lines) are designed to sample the area within one Landsat pixel (30 × 30 m). Results presented in this paper are averaged among subplots and scaled to per-unit-area values. Figure not to scale.

Table A1

Statistical relationships among remote sensing and fuels variables.

Dataset ^a	n	Response variable (y)	Explanatory variable (x)	β_0	(se)	β_1	(se)	adjusted R^2	F-stat _{1,n-2}	P-value
All plots	38	CWD	LandTrendr disturbance magnitude (NBR * 1000)	19.28	(6.07)	0.083	(0.033)	0.127	6.402	0.016
All – 4 error plots ^b	34	CWD	LandTrendr disturbance magnitude (NBR * 1000)	12.27	(5.16)	0.102	(0.026)	0.294	14.720	0.0006
All plots	38	CWD	ADS cumulative presence of WSB and MPB (years)	25.74	(13.59)	0.888	(2.718)	–0.025	0.107	0.746
All – 2 error plots ^c	36	CWD	ADS cumulative presence of WSB and MPB (years)	24.71	(15.67)	1.103	(3.058)	–0.025	0.130	0.721
MH plots	14	CWD	ADS damage by WSB (cumulative defoliation)	14.51	(18.42)	5.424	(3.017)	0.147	3.233	0.097
All plots	38	CWD	ADS damage by MPB (trees per hectare)	34.40	(7.49)	–0.103	(0.134)	–0.011	0.598	0.444
All plots	38	FWD	LandTrendr disturbance magnitude (NBR * 1000)	5.29	(0.80)	0.004	(0.004)	–0.004	0.847	0.364
All plots	38	FWD	ADS cumulative presence of WSB and MPB (years)	1.68	(1.51)	0.879	(0.301)	0.169	8.516	0.006
MH plots	14	FWD	ADS damage by WSB (cumulative defoliation)	5.21	(2.15)	0.394	(0.353)	0.019	1.248	0.286
All plots	38	FWD	ADS damage by MPB (trees per hectare)	4.95	(0.91)	0.020	(0.016)	0.012	1.452	0.236
All plots	38	Forest floor depth	LandTrendr disturbance magnitude (NBR * 1000)	4.47	(0.48)	0.002	(0.003)	–0.011	0.611	0.440
All plots	38	Forest floor depth	ADS cumulative presence of WSB and MPB (years)	4.29	(1.00)	0.094	(0.200)	–0.021	0.223	0.640
MH plots	14	Forest floor depth	ADS damage by WSB (cumulative defoliation)	5.00	(1.21)	0.150	(0.199)	–0.034	0.569	0.465
All plots	38	Forest floor depth	ADS damage by MPB (trees per hectare)	4.98	(0.55)	–0.006	(0.010)	–0.018	0.334	0.567

Notes:

Simple linear regression model for all comparisons: $y = \beta_0 + \beta_1 \cdot x$.Abbreviations and references: CWD: down coarse woody detritus (Mg ha^{-1}); FWD: fine woody detritus (Mg ha^{-1}); Forest floor depth is the sum of litter and duff depth (cm); LandTrendr (Kennedy et al., 2010); NBR: Normalized Burn Ratio (Key & Benson, 2006); ADS: aerial detection survey; WSB: western spruce budworm; MPB: mountain pine beetle.^a Error plots removed where field observations indicated that response variable (e.g., CWD) was not associated with the time interval covered by the LandTrendr or ADS dataset. WSB occurred only at plots in Mt. Hood Zone.^b Model fit shown in Fig. 5b.^c Model fit shown in Fig. 5a.

References

- Balshi, M. S., McGuire, A. D., Duffy, P., Flannigan, M., Walsh, J., & Melillo, J. M. (2009). Assessing the response of area burned to changing climate in western boreal North America using a Multivariate Adaptive Regression Splines (MARS) approach. *Global Change Biology*, 15, 578–600.
- Bentz, B. J., Regniere, J., Fettig, C. J., Hansen, E. M., Hayes, J. L., Hicke, J. A., Kelsey, R. G., Negron, J. F., & Seybold, S. J. (2010). Climate change and bark beetles of the Western United States and Canada: Direct and indirect effects. *Bioscience*, 60, 602–613.
- Brown, J. K. (1974). Handbook for inventorying downed woods material. *USDA Forest Service General Technical Report INT-GTR-16*. Ogden, UT: USDA Forest Service Intermountain Forest and Range Experiment Station.
- Brown, J. K., Oberheu, R. O., & Johnston, C. M. (1982). Handbook for inventorying surface fuels and biomass in the Interior West. *USDA Forest Service General Technical Report INT-GTR-129*. Ogden, UT: USDA Forest Service Intermountain Forest and Range Experiment Station.
- Canty, M. J., Nielsen, A. A., & Schmidt, M. (2004). Automatic radiometric normalization of multitemporal satellite imagery. *Remote Sensing of Environment*, 91, 441–451.
- Carlson, T. N., & Ripley, D. A. (1997). On the relation between NDVI, fractional vegetation cover, and leaf area index. *Remote Sensing of Environment*, 62, 241–252.
- Chavez, P. S., Jr. (1996). Image-based atmospheric corrections - revisited and improved. *Photogrammetric Engineering & Remote Sensing*, 62, 1025–1036.
- Ciesla, W. M. (2006). Aerial signatures of forest insect and disease damage in the western United States. *Forest Health Technology Team, FHTET-01-06*. Ft. Collins, CO: USDA Forest Service.
- Cohen, W. B., & Goward, S. N. (2004). Landsat's role in ecological applications of remote sensing. *Bioscience*, 54, 535–545.
- Cohen, W. B., Yang, Z. G., & Kennedy, R. E. (2010). Detecting trends in forest disturbance and recovery using yearly Landsat time series: 2. TimeSync – Tools for calibration and validation. *Remote Sensing of Environment*, 114, 2911–2924.
- Coops, N. C., Wulder, M. A., & White, J. C. (2006). Integrating remotely sensed and ancillary data sources to characterize a mountain pine beetle infestation. *Remote Sensing of Environment*, 105, 83–97.
- Daly, C., Gibson, W. P., Taylor, G. H., Johnson, G. L., & Pasteris, P. (2002). A knowledge-based approach to the statistical mapping of climate. *Climate Research*, 22, 99–113.
- Dennison, P. E., Brunelle, A. R., & Carter, V. A. (2010). Assessing canopy mortality during a mountain pine beetle outbreak using GeoEye-1 high spatial resolution satellite data. *Remote Sensing of Environment*, 114, 2431–2435.
- Eidenshink, J., Schwind, B., Brewer, K., Zhu, Z. L., Quayle, B., & Howard, S. (2007). A project for monitoring trends in burn severity. *Fire Ecology*, 3, 3–21.
- Fleming, R. A., Candau, J. N., & McAlpine, R. S. (2002). Landscape-scale analysis of interactions between insect defoliation and forest fire in Central Canada. *Climatic Change*, 55, 251–272.
- Franklin, S. E., Waring, R. H., McCreight, R. W., Cohen, W. B., & Fiorella, M. (1995). Aerial and satellite sensor detection and classification of western spruce budworm defoliation in a subalpine forest. *Canadian Journal of Remote Sensing*, 21, 299–308.
- Geiszler, D. R., Gara, R. I., Driver, C. H., Gallucci, V. F., & Martin, R. E. (1980). Fire, fungi, and beetle influences on a lodgepole pine ecosystem of south-central Oregon. *Oecologia*, 46, 239–243.
- Goheen, E. M., & Willhite, E. A. (2006). Field guide to common diseases and insect pests of Oregon and Washington conifers. *R6-NR-FID-PR-01-06, USDA Forest Service Pacific Northwest Region, Portland, OR* (327 pp.).
- Goodwin, N. R., Coops, N. C., Wulder, M. A., Gillanders, S., Schroeder, T. A., & Nelson, T. (2008). Estimation of insect infestation dynamics using a temporal sequence of Landsat data. *Remote Sensing of Environment*, 112, 3680–3689.
- Goodwin, N. R., Magnussen, S., Coops, N. C., & Wulder, M. A. (2010). Curve fitting of time-series Landsat imagery for characterizing a mountain pine beetle infestation. *International Journal of Remote Sensing*, 31, 3263–3271.
- Harmon, M. E., & Sexton, J. (1996). *Guidelines for measurements of woody detritus in forest ecosystems*. Publication no. 20. University of Washington, Seattle, WA: US LTER Network Office, 73 p.
- Hudiburg, T., Law, B. E., Turner, D. P., Campbell, J. L., Donato, D. C., & Duane, M. (2009). Carbon dynamics of Oregon and Northern California forests and potential land-based carbon storage. *Ecological Applications*, 19, 163–180.
- Hummel, S., & Agee, J. K. (2003). Western spruce budworm defoliation effects on forest structure and potential fire behavior. *Northwest Science*, 77, 159–169.
- Kennedy, R. E., Yang, Z. G., & Cohen, W. B. (2010). Detecting trends in forest disturbance and recovery using yearly Landsat time series: 1. LandTrendr – Temporal segmentation algorithms. *Remote Sensing of Environment*, 114, 2897–2910.
- Key, C. H., & Benson, N. C. (2006). Landscape assessment: Ground measure of severity, the composite burn index; and remote sensing of severity, the Normalized Burn Ratio. *FIREMON: Fire effects monitoring and inventory system. USDA Forest Service General Technical Report RMRS-GTR-164-CD*. Fort Collins, CO: USDA Forest Service Rocky Mountain Research Station.
- Klutsch, J. G., Negron, J. F., Costello, S. L., Rhoades, C. C., West, D. R., Popp, J., & Caissie, R. (2009). Stand characteristics and downed woody debris accumulations associated with a mountain pine beetle (*Dendroctonus ponderosae* Hopkins) outbreak in Colorado. *Forest Ecology and Management*, 258, 641–649.
- Kurz, W. A., Dymond, C. C., Stinson, G., Rampley, G. J., Neilson, E. T., Carroll, A. L., Ebata, T., & Safranyik, L. (2008). Mountain pine beetle and forest carbon feedback to climate change. *Nature*, 452, 987–990.
- Littell, J. S., Oneil, E. E., McKenzie, D., Hicke, J. A., Lutz, J. A., Norheim, R. A., & Elsner, M. M. (2010). Forest ecosystems, disturbance, and climatic change in Washington State, USA. *Climatic Change*, 102, 129–158.
- Logan, J. A., Regniere, J., & Powell, J. A. (2003). Assessing the impacts of global warming on forest pest dynamics. *Frontiers in Ecology and the Environment*, 1, 130–137.
- Lynch, H. J., & Moorcroft, P. R. (2008). A spatiotemporal Ripley's K-function to analyze interactions between spruce budworm and fire in British Columbia, Canada. *Canadian Journal of Forest Research*, 38, 3112–3119.
- Lynch, H. J., Renkin, R. A., Crabtree, R. L., & Moorcroft, P. R. (2006). The influence of previous mountain pine beetle (*Dendroctonus ponderosae*) activity on the 1988 Yellowstone fires. *Ecosystems*, 9, 1318–1327.
- Meigs, G. W., Donato, D. C., Campbell, J. L., Martin, J. G., & Law, B. E. (2009). Forest fire impacts on carbon uptake, storage, and emission: The role of burn severity in the Eastern Cascades, Oregon. *Ecosystems*, 12, 1246–1267.
- Negron, J. F., Bentz, B. J., Fettig, C. J., Gillette, N., Hansen, E. M., Hays, J. L., Kelsey, R. G., Lundquist, J. E., Lynch, A. M., Progar, R. A., & Seybold, S. J. (2008). US Forest Service bark beetle research in the western United States: Looking toward the future. *Journal of Forestry*, 106, 325–331.
- Nelson, T., Boots, B., & Wulder, M. A. (2006). Large-area mountain pine beetle infestations: Spatial data representation and accuracy. *The Forestry Chronicle*, 82, 243–252.
- Page, W., & Jenkins, M. J. (2007). Mountain pine beetle-induced changes to selected lodgepole pine fuel complexes within the intermountain region. *Forest Science*, 53, 507–518.

- Page, W., & Jenkins, M. J. (2007). Predicted fire behavior in selected mountain pine beetle infested lodgepole pine. *Forest Science*, 53, 662–674.
- R Development Core Team (2011). *R: A language and environment for statistical computing*. Vienna, Austria: R Foundation for Statistical Computing. <http://R-project.org>.
- Raffa, K. F., Aukema, B. H., Bentz, B. J., Carroll, A. L., Hicke, J. A., Turner, M. G., & Romme, W. H. (2008). Cross-scale drivers of natural disturbances prone to anthropogenic amplification: The dynamics of bark beetle eruptions. *Bioscience*, 58, 501–517.
- Russell, R. E., Saab, V. A., Dudley, J. G., & Rotella, J. J. (2006). Snag longevity in relation to wildfire and postfire salvage logging. *Forest Ecology and Management*, 232, 179–187.
- Simard, M., Romme, W. H., Griffin, J. M., & Turner, M. G. (2011). Do mountain pine beetle outbreaks change the probability of active crown fire in lodgepole pine forests? *Ecological Monographs*, 81, 3–24.
- Swetnam, T. W., & Lynch, A. M. (1993). Multicentury, regional-scale patterns of western spruce budworm outbreaks. *Ecological Monographs*, 63, 399–424.
- Teillet, P. M., Staenz, K., & Williams, D. J. (1997). Effects of spectral, spatial, and radiometric characteristics on remote sensing vegetation indices of forested regions. *Remote Sensing of Environment*, 61, 139–149.
- Verbesselt, J., Robinson, A., Stone, C., & Culvenor, D. (2009). Forecasting tree mortality using change metrics derived from MODIS satellite data. *Forest Ecology and Management*, 258, 1166–1173.
- Vogelmann, J. E., Howard, S. M., Yang, L. M., Larson, C. R., Wylie, B. K., & Van Driel, N. (2001). Completion of the 1990s National Land Cover Data Set for the conterminous United States from Landsat thematic mapper data and ancillary data sources. *Photogrammetric Engineering and Remote Sensing*, 67, 650–662.
- Vogelmann, J. E., Tolk, B., & Zhu, Z. L. (2009). Monitoring forest changes in the south-western United States using multitemporal Landsat data. *Remote Sensing of Environment*, 113, 1739–1748.
- Westerling, A. L., Hidalgo, H. G., Cayan, D. R., & Swetnam, T. W. (2006). Warming and earlier spring increase western US forest wildfire activity. *Science*, 313, 940–943.
- Wulder, M. A., Dymond, C. C., White, J. C., Leckie, D. G., & Carroll, A. L. (2006). Surveying mountain pine beetle damage of forests: A review of remote sensing opportunities. *Forest Ecology and Management*, 221, 27–41.